

Universal set of Observables for the Koopman Operator through Causal Embedding

G Manjunath and A de Clercq

Department of Mathematics & Applied Mathematics, University of Pretoria, Pretoria 0028

Email: manjunath.gandhi@up.ac.za & adriaandeclercq1998@gmail.com

Abstract

Obtaining repeated measurements from physical and natural systems for building a more informative dynamical model of such systems is engraved in modern science. Results in reconstructing equivalent chaotic dynamical systems through delay coordinate mappings, Koopman operator based data-driven approach and reservoir computing methods have shown the possibility of finding model equations on a new phase space that is relatable to the dynamical system generating the data. Recently, rigorous results that point to reducing the functional complexity of the map that describes the dynamics in the new phase have made the Koopman operator based approach very attractive for data-driven modeling. However, choosing a set of nonlinear observable functions that can work for different data sets is an open challenge. We use driven dynamical systems comparable to that in reservoir computing with the *causal embedding property* to obtain the right set of observables through which the dynamics in the new space is made equivalent or topologically conjugate to the original system. Deep learning methods are used to learn a map that emerges as a consequence of the topological conjugacy. Besides stability, amenability for hardware implementations, causal embedding based models provide long-term consistency even for maps that have failed under previously reported data-driven or machine learning methods.

Keywords Data-driven dynamical systems, Koopman's theory, Causal Embedding, Nonautonomous Dynamical Systems.

Performing experimental measurements on biological, physical, and artificial systems to obtain a more informative dynamical model has been well established in modern day science. The practical purpose of obtaining high fidelity models for instance in climate science is not only for forecasting or for the study of attractors as better forecasting indeed helps both manage better service interruptions and resource management, but for understanding the response of statistical properties of the perturbations of models that has very promising applications (e.g., [1, 2] and references therein). Although attempts made to build model equations from complex data such as sunspot cycles date

back to the 1920s in [3], a major breakthrough came through the Takens embedding theorem [4] that made state-space reconstruction a valuable tool for any kind of analysis. Since experimental measurements of such systems are not directly the system’s states, but a univariate or a multivariate time-series whose span is smaller than the system’s dynamics, Takens theorem under some generic conditions establishes the learnability of a system that is equivalent (topologically conjugate) from which the observed time-series was derived. While this topological result ensures an alternate representation, the quality of the representation remains sensitive to various parameters such as the experimental measurement error or noise, continuous spectra, nature of the attractor, and the delay or the number of time-lags chosen, and importantly, stability of the embedding – moreover global approximation techniques that generate a single map that fits the data often work well only for functions with low functional complexity, i.e., functions that are nice enough so that they can be accurately approximated by machine learning procedures, therefore calling for extensive adaptations. An example of such a problem is where neural networks often fail to learn the attractor in the reconstructed space as shown in [5].

Although not theoretically assuring accurate reconstruction as in Takens delay embedding, the more recent approaches in machine learning that employ the reservoir computing paradigm [6, 7] and data-driven algorithms based on Koopman’s theory [8, 9] have shown greater quantitative accuracy in forecasting than what has been achieved through delay-embedding alone. The prominent idea in reservoir computing approaches is to transform the available temporal data into another higher dimensional space through the dynamics of a driven dynamical system (e.g., [10, 11]). The driven dynamical system’s state is then post-processed to fit the prediction task by training only a few weights. Although there is no theoretical framework that guarantees the existence of a post-processing function, it is approximated typically by a linear regression. These methods often give good short-term predictions but fail to learn the attractor for many chaotic systems [12, 13, 14, 15].

The idea behind Koopman’s theory is to transform observed data sample-wise generated from an unknown dynamical system into a new space or a new coordinate system so that the induced dynamics in the new coordinate system can be approximated by a more simple set of equations, for instance by a linear system of equations. The popular algorithms like Dynamic Mode Decomposition and Extended-Dynamic Mode Decomposition [16, 17] involves a priori determination of a Koopman invariant subspace obtained by a handpicked choice of observables. If the observables and the Koopman invariant subspace they determine is not adequate enough to capture some essential dynamics, the resultant approximation to the Koopman operator is poor, and hence the qualitative behavior like the phase portrait of the forecasted data veers down to a different one in a very few time-steps. In any case for forecasting chaotic data, linear systems in finite-dimensions cannot be topologically equivalent to a linear map, and hence such methods are limited in performance while modeling complex/chaotic data.

Balancing model complexity with accuracy has recently led to the idea of sparse representations where a vector field of a differential equation that describes the dynamics is approximated by an optimal linear combination of a very few functions that are ‘possibly nonlinear’ from a chosen library. Such representations have yielded not only accurate prediction results for some class of chaotic systems but can be used to build simpler model equations from data [18, 19].

The library is determined by insights into the physics of the model, and the performance of such modeling is affected in the absence of such physical precognition. Library free approaches such as combining delay-embedding and Koopman theory allows to build intermittently forced linear models [20]. However, unlike Takens embedding the existing reservoir computing or data-driven methods do not ensure of finding an equivalent (conjugate) model of the data. In the case of Koopman analysis, by capturing a portion of the spectrum like the eigenvalues of the operator, only a topological semi-conjugacy can be obtained. Although there is talk about finding faithful representations in the Koopman framework leading to topological conjugacy [21] there is currently no framework that guarantees existence or a method to find them.

On the positive side, generalization of Takens embedding (e.g., [22, 23, 24, 25], and notably [25, Theorem 1], generic continuous-time-lagged observations of attractors of homeomorphisms on compact spaces are sufficient for attractor reconstruction. On preserving the geometry of the reconstructed attractor, some recent theoretical and empirical studies suggest that it may be possible to construct delay embeddings that are not only homeomorphic or diffeomorphic to the original system but nearly isometric [22, 26]. Isometric embeddings for instance obtained by the Nash embedding theorem help preserving local neighborhoods of points on the attractor, a geometric feature desired during forecasting and reconstructing attractors. More recent studies are suggestive that for large enough time-lagged observations [27, 28] isometric embeddings can be obtained.

In the spirit of obtaining an isometric embedding through large, perhaps infinite, time-lagged observations we employ a driven dynamical system with a certain property called the causal embedding to transform the temporal data onto another sequence in a different space. Remarkably, the infinite-delay maps induced by such dynamical systems determine the observables for the Koopman operator of the inverse-limit space (e.g., [29]) of the dynamical system generating the data. This, in conclusion, gives a topological conjugacy – this solves the problem of finding a finite faithful raised in [21]. Also, causal embedding renders the temporal data to be mapped as a nonautonomous uniform attractor in the new phase space and that goes beyond stable embedding in Takens embedding since every orbit is stably mapped as well. Further empirical evidence shows that a linearity measure like a Pearson correlation coefficient indicates that if the dimension of the new space is larger than the linear relationship in successive times of the transformed sequence is larger than in the given data. Furthermore, using a generalization of the Pearson correlation coefficient [30], empirical evidence shows a better correlation between successive terms in the higher dimensional embedded space. This helps to learn a simpler global approximation to the data that was not always guaranteed by applying Takens delay embedding. In summary, we can find a model that is topologically conjugate to the unknown system with lesser nonlinearity and have its dynamics robust to noise and model parameters. We present a methodology guided by theoretical evidence to achieve these objectives and obtain long-term consistency in learning models from chaotic data. The long-term topological and statistical consistency achieved is much higher than previously reported in the field of delay-embedding, reservoir computing, and Koopman’s theory. Moreover, the methodology does not require selecting a library of functions or observable but allows for an arbitrary choice of the driven dynamical system satisfying the causal embedding property. Such driven dynamical systems with the causal embedding property are a special subclass of driven systems that have already been employed in dedicated hardware involving neuromorphic or reservoir computing (e.g., [31, 32, 33]).

Causal Embedding and Learning

A dynamical system in this work is a space (U, T) where U is a compact metric space and $T : U \rightarrow U$ is a function (that is not necessarily continuous). Henceforth, we consider only surjective dynamical systems, i.e., systems for which T is surjective. In fact, if A is any invariant set, i.e., if $T(A) := \cup_{u \in A} Tu = A$, then T is surjective on A , so if T is not surjective to start with we can restrict it to an invariant set. We call any sequence $\bar{u} = \{u_n\}_{n \in \mathbb{Z}}$ that obeys the update equation, $u_{n+1} = Tu_n$ where $n \in \mathbb{Z}$ as an orbit of T .

The problem of forecasting a dynamical system involves predicting u_{m+1}, u_{m+2}, \dots given the finite segment of an orbit u_0, u_1, \dots, u_m . A problem of learning a dynamical system involves learning T or learn model equations that not only can be used to regenerate the data but also is equivalent to that of T . A core concept in dynamical systems theory is the notion of equivalent dynamical systems. Finding an equivalent dynamical system to (U, T) means finding another dynamical system (V, S) so that there exists a homeomorphism $\phi : U \rightarrow V$ with the property that $\phi \circ T = S \circ \phi$. Such a map ϕ is called a conjugacy and we say that (V, S) is conjugate to (U, T) . If we relax the condition on ϕ where, instead of having a homeomorphism, we only require ϕ to be continuous, then we call ϕ a semi-conjugacy and say the systems are semi-conjugate. A system being conjugate to the original means that there is a one-to-one correspondence between the two systems, whereas a semi-conjugacy when it is many-to-one mapping provides a coarse-grained description of the original system. When (V, S) is semi-conjugate to (U, T) then it is customary to say that (V, S) is a factor of (U, T) or that (U, T) is an extension of (V, S) .

Given a segment of an orbit (U, T) , our approach in this paper is to build model equations of a system that is topologically conjugate to an extension of (U, T) . To define such an extension, we first let the left-infinite countable cartesian product of U be denoted by $\overleftarrow{U} := \dots \times U \times U$ (and equip it with the product topology). Any dynamical system (U, T) (since we assume T is surjective) determines a nonempty subspace \hat{U}_T of \overleftarrow{U} given by

$$\hat{U}_T := \{(\dots, u_{-2}, u_{-1}) : Tu_n = u_{n+1}\},$$

and \hat{U}_T is equivalent to the inverse limit space of (U, T) or the natural extension of (U, T) in the literature (e.g., [29]). The map T also induces a self-map \hat{T} on \hat{U}_T defined by $\hat{T} : (\dots, u_{-2}, u_{-1}) \mapsto (\dots, u_{-2}, u_{-1}, T(u_{-1}))$. It is straightforward to find that the surjective dynamical system (U, T) is semi-conjugate to (\hat{U}_T, \hat{T}) and whenever, (U, T) is invertible, (\hat{U}_T, \hat{T}) is conjugate to (U, T) .

To build an equivalent model of (\hat{U}_T, \hat{T}) , our idea is to embed \hat{U}_T in a space X . This can be asymptotically achieved through a driven dynamical system when an element of \hat{U}_T that is a left-infinite sequence of U is fed sequentially as the drive or the input. We first disregard the map T and define a driven dynamical system or a driven system in short. This driven system comprises an input metric space (U, d_U) , a compact metric (state) space (X, d) and a **continuous function** $g : U \times X \rightarrow X$. For brevity, we refer to g as a driven system with all underlying entities quietly understood. Since X is assumed to be compact, it follows [34] that for every bi-infinite sequence \bar{u} there exists at least one sequence $\{x_n\}$ that satisfies $x_{n+1} = g(u_n, x_n)$ for all $n \in \mathbb{Z}$ when the

elements of \bar{u} are fed sequentially. Any such bi-infinite sequence $\{x_n\}$ is called a solution of g for the input \bar{u} . In particular, if we denote a bi-infinite sequence $\{u_n\}_{n \in \mathbb{Z}} \subset U$ by \bar{u} , and its left-infinite part $\tilde{u}^n := (\dots, u_{n-2}, u_{n-1})$, and we note that \tilde{u}^n belongs to \overleftarrow{U} regardless of $n \in \mathbb{Z}$.

We next identify a subspace X_U of X that contains all possible solutions into which we aim to embed \widehat{U}_T . To realize such a subspace of a driven system g , we again discard T and define the *reachable set* of the driven system g to be the union of all the elements of all the solutions, i.e.,

$$X_U := \left\{ x \in X : \exists \text{ a solution } \{x_n\} \text{ for some } \bar{u} \text{ \& } x = x_k \text{ for some } k \in \mathbb{Z} \right\}.$$

For example, when $U = [0, 1]$ and $X = [0, 1]$, for the driven system $g(u, x) := \frac{ux}{2}$ regardless of any sequence in U , $x_n \equiv 0$ for $n \in \mathbb{Z}$ is the only solution of g , and hence the reachable set $X_U = \{0\}$. It is not possible to embed a inverse limit space \widehat{U}_T with more than one element in $\overleftarrow{X_U}$. To achieve a desired embedding we would consider driven systems that are also state-input invertible (SI-invertible). We say g is SI-invertible if $g(\cdot, x) : U \rightarrow X$ is invertible for all x , i.e., if the current state x_n and the future state x_{n+1} are given then the current input u_n can be uniquely determined, since the inverse of $g(\cdot, x_n)$ exists. For instance, consider a recurrent neural network (RNN) with N artificial neurons and $U \subset \mathbb{R}^N$ and $X = [-1, 1]^N$ (the cartesian product of N copies of $[-1, 1]$) given by

$$g(u, x) = (1 - a)x + \overline{\text{atanh}}(Au + \alpha Bx), \quad (1)$$

where A is a $N \times N$ matrix with input connections call the input matrix and the matrix B is also of dimension $N \times N$ representing the strength of the interconnections called a reservoir matrix, and a and α are real-valued parameter that are normally called leak rate and scaling of the reservoir B respectively and $\overline{\text{atanh}}(*)$ is (the nonlinear activation) \tanh performed component-wise on $*$. The RNN accepts inputs of vectors with N elements, and if an input v_n is of dimension $K < N$, one can pad $N - K$ zeroes to obtain an input of dimension K i.e., $v_n \mapsto (v_n^1, v_n^2, \dots, v_n^K, 0, 0, \dots, 0) = u_n$. It can be easily verified that when both A and B are invertible, then g has SI-invertibility.

When g is SI-invertible, we define a relation on X_U (a subset defined on $X_U \times X_U$) by $Y_T := \{(x_{n-1}, x_n) : \{x_k\}_{k \in \mathbb{Z}} \text{ is a solution for some orbit of } T \text{ and } n \in \mathbb{Z}\}$ called the induced-relation of (U, T) . It easily follows [34] that there exists a map $G_T : Y_T \rightarrow Y_T$ defined by $(x_{n-1}, x_n) \mapsto (x_n, x_{n+1})$.

In general, there could be no well-founded relationship between the dynamics of the maps T and G_T . For a driven system g , since the solution depends both on the input and g itself. We now establish a relationship between the mapping G_T and the dynamical system T for a class of driven dynamical systems. First, we pause to ask if the complexity of the solution of g can remain unaffected in the sense if when a new input value v appears at time n , i.e., symbolically if $\tilde{u}^n v := (\dots, u_{n-2}, u_{n-1}, v)$ is the input up to time n , the mapping $\sigma_v : \tilde{u}^n \mapsto \tilde{u}^n v$ satisfies the following commutativity diagram for some continuous map $h : \overleftarrow{U} \rightarrow X_U$ which we call an universal semi-conjugacy holds:

$$\begin{array}{ccc} \overleftarrow{U} & \xrightarrow{\sigma_v} & \overleftarrow{U} \\ h \downarrow & & \downarrow h \\ X_U & \xrightarrow{g(v, \cdot)} & X_U. \end{array} \quad (2)$$

The above commutativity holds whenever g satisfies the unique solution property – we say a driven system g has the unique solution property (USP) if for each input \bar{u} there exists exactly one solution. In other words, g has the USP if there exists a well-defined solution-map Ψ so that $\Psi(\bar{u})$ denotes the unique solution obtained from the input \bar{u} . Conversely, whenever the diagram in (2) commutes the system g has the USP [35] and $h(\tilde{u}^k) = x_k$, where x_k is the value of the solution. In our context, the USP is equivalent to saying g is a topological contraction [34] and this notion is independent of SI-invertibility. This topological contraction is commonly called as the echo state property [10], and systems with this property have other important properties [36, 11].

For a driven system g with the USP and if the mapping $H : \overleftarrow{U} \rightarrow \overleftarrow{X}_U$ defined by $H(\bar{u}) := (\dots, h(r^2\bar{u}), h(r\bar{u}), h(\bar{u}))$ turns out to be an embedding of \overleftarrow{U} in \overleftarrow{U} , then we call H a causal embedding. When g has the USP and is SI-invertible [34], then g has the causal embedding property. In the particular case, where the input is an orbit of a dynamical system (U, T) and g has the causal embedding property, then it follows from (2), that $\sigma_{Tu_{-1}}$ is \hat{T} (see [34]), and by considering just two component functions of H , i.e., with $H_2(\bar{u}) := (h(r\bar{u}), h(\bar{u}))$ (strictly speaking, it is H_2 restricted to \hat{U}_T) the following diagram (printed in black) commutes:

$$\begin{array}{ccc}
 \hat{U}_T & \xrightarrow{\hat{T}} & \hat{U}_T \\
 \downarrow H_2 & & \downarrow H_2 \\
 H_2(\hat{U}_T) & \xrightarrow{G_T} & H_2(\hat{U}_T) \\
 & \searrow (\Gamma, \pi_2) & \nearrow (\pi_2, g) \\
 & U \times X. &
 \end{array} \tag{3}$$

It is remarkable, that a driven system with the causal embedding property produces a mapping H_2 that embeds the inverse limit space of any dynamical system defined on U or a subspace of U . Now we list the consequences of the commutativity in (3). When g is SI-invertible and $\{u_n\} \subset U$ is an orbit of an dynamical system (U, T) , the following results proved in [34] hold: (i) there exists a map $G_T : Y_T \rightarrow Y_T$ defined by $(x_{n-1}, x_n) \mapsto (x_n, x_{n+1})$ (ii) further, if g has the USP then (Y_T, G_T) is topologically semi-conjugate to (\hat{U}, \hat{T}) (iii) finally, if $T : U \rightarrow U$ is a homeomorphism, then (Y_T, G_T) is topologically conjugate to (\hat{U}, \hat{T}) (and hence also conjugate to (U, T)). The existence of the topological semi-conjugacy in (ii) and topological conjugacy and (iii) is due to the causal embedding property of g , and $H_2(\bar{u}) := (h(r\bar{u}), h(\bar{u}))$. Since two successive points (x_{n-1}, x_n) of a solution of g with input \bar{u} lie in Y_T , one can learn the map $G_T : (x_{n-1}, x_n) \mapsto (x_n, x_{n+1})$ through a finite segment (x_0, \dots, x_n) . The value of x_{n+k} in x_n, x_{n+1}, \dots can be found through repeated application of G_T on two previous values (x_{n+k-2}, x_{n+k-1}) . Since g is SI-invertible, one can find u_n since $u_n = g_{*, x_n}^{-1}(x_{n+1})$ for each n , and one can forecast u_n, u_{n+1}, \dots . As long as g has the causal embedding property, the mapping H_2 can embed the inverse-limit space of any dynamical system defined by a homeomorphism $T : U \rightarrow U$ into $X_U \times X_U$. Thus, one needs to learn only G_T for a specific T .

Prior to discussing learning the map G_T , we note that the map H_2 transforms temporal data \tilde{u} onto the space $X_U \times X_U$. The idea of transforming data to a different space is also explored in Koopman’s theory, and we bring out the connection to Koopman’s theory next. Given a dynamical system (U, T) and some vector space V of functions f whose domain is U , the operator $\mathcal{K} : V \rightarrow V$ so that $\mathcal{K}f = f \circ T$ holds is called the Koopman operator. Since V is a vector space, in Koopman’s theory the study of dynamics reduces to the study of linear operators on function spaces. It is customary to consider a class of observables where V is some Hilbert space or some L^p space, i.e., an observable f represents an equivalence class of measurable functions. The central idea of using Koopman’s theory for forecasting dynamical systems is to obtain a collection of observables $\mathbf{f} = \{f_1, \dots, f_N\}$ so that the dynamics in \mathbb{R}^N can be approximated by a simpler map, say F . The choice of the L^p space considered determines the spectrum of the Koopman operator \mathcal{K} , and if the span of the observables is invariant under \mathcal{K} , one captures a portion of the spectrum of \mathcal{K} through the map F (e.g., [37]). When (Y_T, G_T) is topologically conjugate to (\hat{U}, \hat{T}) , and $X \subset \mathbb{R}^N$, the component functions of H_2 determines a set of \mathbb{R}^2 -valued observables of the inverse-limit space (\hat{U}, \hat{T}) that goes beyond the approximation of the spectrum of the Koopman operator induced by \hat{T} by determining the values of the Koopman operator on these observables, i.e., when $X = \mathbb{R}^N$, then the map G_T defined above is a self-map on a subset of $\mathbb{R}^N \times \mathbb{R}^N$ and if $\pi_i : \mathbb{R}^N \rightarrow \mathbb{R}^2$ is the i th coordinate projection then $\mathcal{K}f_i = \pi_i \circ G_T \circ H_2$, where \mathbf{f} comprises the coordinate functions of H_2 taking values in \mathbb{R}^2 . In some recent applied Koopmanism language, \mathbf{f} the component functions of H_2 and the map G_T together form a finite faithful representation [21]. Forecasting the observed values of H_2 is possible by learning the map G_T , and although we do not have an explicit algebraic expression for H_2 that is not essential to forecast the input sequence since $H_2(\tilde{u}^n)$ determines u_{n-1} uniquely as g is SI-invertible.

The advantages of allowing a driven system determine the observables, i.e., the components of the function $H_2 : \hat{U}_T \rightarrow X_U \times X_U$ has a distinct advantage over selecting or optimizing the choice of observables as in the Extended-Dynamic Mode Decomposition algorithm [16, 17]. We can alter the functional complexity of G_T by raising the number of observables or equivalently by altering the dimension of X – in the case of an RNN implementation of g , by simply changing the number of neurons in the network. Empirically, increasing the dimension of X is found to increase the linear relationship that is measured as a generalization of the Pearson correlation coefficient to random vectors (e.g., [30]) between (x_{n-1}, x_n) and $G_T(x_{n-1}, x_n)$, and such numerical evidence is tabulated in [34, Table]. The estimation of such linear relationship in [34, Table] obtained by measurements alone is justified whenever $\{u_n\}$ is a realization of an ergodic process since then when g has the USP, any solution $\{x_n\}$ is also a realization of an ergodic process [38], and hence the generalized Pearson correlation coefficient between (x_{n-1}, x_n) and $G_T(x_{n-1}, x_n)$ is independent of n . In contrast, expanding the set of observables in Koopman’s theory with the aim of learning a map with a less functional complexity is a highly involved task, not least because so much one often does not know how to guess a new observable, but adding observables does not necessarily retain the invariance of the span of the observables under the Koopman operator. Also, the spectrum of the Koopman operator of conjugate systems are identical while the spectrum of the Koopman operator of a factor is contained in its extension (e.g. [39]). Hence the spectrum of the Koopman operator of G_T contains that of the Koopman operator of T . These spectra are equal when T is a homeomorphism. Lastly, the component functions of H_2 would not change with the dynamical system as long as it is defined on U , and hence we have a universal set of observables for all dynamical systems defined on U .

Equations from Data and Forecasting

In principle, feeding an orbit of (U, T) to a driven system that is SI-invertible and has USP enables learning the map G_T from the simulated solution so that the digram in (3) commutes. However, one can learn G_T indirectly by first learning the map $\Gamma : (x_{n-1}, x_n) \mapsto u_n$ – the map Γ always exists when G_T exists (see [34]). Then since $(\Gamma, \pi_2)(x_{n-1}, x_n) = (u_n, x_n)$ where π_2 is the coordinate projection (see the red print of the commutativity diagram in (3) or that in Fig. 1A), one can feed u_n back to the driven system to obtain the following system of equations that describes a self-map S on a subset of $U \times X$ by

$$u_{k+1} = \pi_1 \circ (\Gamma, \pi_2) \circ (\pi_2, g)(u_k, x_k) \quad (4)$$

$$x_{k+1} = \pi_2 \circ (\Gamma, \pi_2) \circ (\pi_2, g)(u_k, x_k). \quad (5)$$

Equation (4) per se represents a (possibly nonlinear) difference equation of infinite order since $x_k = h(\tilde{u}^k)$. The variable x_k acts as an auxiliary variable in the system defined by S . The advantages of employing (4)-(5) instead of learning G_T are the following: (i). we can save resources by learning Γ instead of G_T since the target u_n sans the padded zeroes is of a much smaller dimension than that of X in practice (ii). if \tilde{u} and its noisy version \tilde{v} are nearby then their tails could be significantly different in the product topology. Also, in that case, $h(\tilde{u})$ and $h(\tilde{v})$ are nearby owing to the (uniform) continuity of h , and thereby providing robustness to input noise and minimizing the effect of errors made in the distant past. This is referred to as input-related stability [11, Theorem 3.1]. More precisely, $h(\tilde{u})$ is affected to an arbitrarily small extent by that left-infinite segment of the past of the input beyond some arbitrarily large but finite time. (iii). If T is chaotic, then \hat{T} is also chaotic and the map S on a domain D contained in $U \times X$ is also chaotic. This entails a small open ball of initial conditions contained in $U \times X$ to grow quickly in time. Separately, due to either noise in the input or due to approximation of Γ by its learnt version, the noise could expand the domain of the map S beyond D . We note that g can be designed so that the solutions of g is always in the compact space X regardless of the expansion of the input space U (for e.g., (1)). Hence the dynamics that spills much beyond D can be quenched by a saturation function like in the RNN in (1). This restricts the growth of the error while forecasting. With an RNN in (1), the set $H_2(\hat{U}_T)$ can be made to expand by setting α large enough while retaining the USP [34]) so that the quenching gets close to the boundary of the domain of S . (iv) when a parameter λ is such that $\lambda \mapsto g_\lambda$ is continuous the universal semi-conjugacy h_λ is also continuous with respect to the parameter λ . This is referred to as parameter-related stability [11, Theorem 3.2], a consequence of the USP.

The solutions of g are non-autonomous uniform attractors, that is each solution attracts all other initial conditions towards the components of the solution, and this attractivity is uniform for all solutions – uniform attraction property [35]. This also ensures that if we initialize the driven system with an arbitrary initial value $y_m \in X$, then the sequence $y_{m+1}, y_{m+2}, y_{m+3}, \dots$ satisfying $y_{k+1} = g(u_k, y_k)$ for $k \geq m$ approximates the actual solution $\{x_n\}$ uniformly. To be precise, given $\epsilon > 0$ (independent of y_m) there is an integer n so that the distance between x_{n+i} and y_{n+i} is less than ϵ for all $i \geq 0$, where $\{x_m\} = \Psi(\tilde{u})$ and y_{n+i} is generated by $y_{k+1} = g(u_k, y_k)$ for $k \geq m$. This is a property of g and hence the same convergence to the actual solution holds after learning Γ in (4)-(5). In contrast, the Takens delay embedding theorem in [4] does not guarantee a stable embedding,

and in particular the attractor embedded is not necessarily an attractor in the reconstructed space. Theoretical conditions under which a kind of stable embedding can be obtained depends actually on the observables used in the delay-coordinate mapping [27].

We next consider a more general problem of learning a dynamical system when only observations of an orbit are available. To be explicit, if (W, T) is a dynamical system with dynamics generated by $w_{n+1} = Tw_n$, and if $\theta : W \rightarrow \mathbb{R}$ is an observable, then the task is to learn a system that is topologically conjugate to (W, T) and predict $\theta(w_{m+1}), \theta(w_{m+2}), \dots$ using the data $\theta(w_0), \theta(w_1), \dots, \theta(w_m)$. Suppose the input from the delay-coordinate map $\Phi_{\theta, 2d}(\theta(w_n)) := (\theta(w_{n-2d}), \dots, \theta(w_{n-1}), \theta(w_n))$ is fed into the driven system as u_n . Then it is straightforward to establish that whenever $\Phi_{\theta, 2d}$ is a topological conjugacy between the unknown system (W, T) and $(\Phi_{\theta, 2d}(W), F)$, where F is a homeomorphism for instance as in Takens delay embedding, and g has the causal embedding property. Since F is a homeomorphism on $\Phi_{\theta, 2d}(W)$, by replacing F by T in (3) we obtain G_T that is topologically conjugate to the inverse-limit system of $(\Phi_{\theta, 2d}(W), F)$ (see [34]). Also, when $X \subset \mathbb{R}^N$, the component functions of H_2 are the set of observables of the inverse-limit system of $(\Phi_{\theta, 2d}(W), F)$ on which the action of the Koopman operator can be learnt from data.

In the above scenario, we had assumed that the delay used in the delay-coordinates is sufficient for a map F to exist. However in the case when the required delay is not known, we demonstrate appealing numerical results later in the article, but the theory is based on a conjecture. If the component functions of H_2 form sufficiently large number of “independent” functions so that it can embed $\Theta(\widehat{W}) := \{\dots, \theta(w_{-2}), \theta(w_{-1}) : w_{n+1} = Tw_n\}$ in $X_U \times X_U$ then we can learn a map G_T by feeding $\theta(w_0), \theta(w_1), \dots, \theta(w_m)$ into the driven system g . This can be explained as follows. If the conjecture that H_2 can embed $\Theta(\widehat{W})$ in $X_U \times X_U$ is true then there is a homeomorphism $\tilde{F} := (\dots, \theta(w_{k-2}), \theta(w_{k-1})) \mapsto (\dots, \theta(w_{k-1}), \theta(w_k))$ owing to the Takens embedding theorem. If for instance θ and (W, T) satisfy the hypotheses of Takens delay embedding theorem then such a mapping \tilde{F} exists [34] and then we can define $G_T : (x_{n-1}, x_n) \mapsto (x_n, x_{n+1})$ also by $G_T = H_2 \circ \tilde{F} \circ H_2^{-1}$. It can be shown that the component functions of H_2 are also sufficiently smooth when g has the USP and sufficiently smooth in view of a known result [40, Theorem III.1]. If U is a smooth manifold of dimension M , and there are at least $2M + 1$ component functions of H_2 that are generic in the sense of Whitney’s embedding theorem – then H_2 would embed $\Theta(\widehat{W})$ in $X_U \times X_U$. However, it is an open question whether h (and hence $o H_2$) comprise such functions that are generic in the sense of Whitney, and the only result we currently the authors are aware of is that h restricted to $\Theta(\widehat{W})$ turns out to be the so-called echo state map is a limit point of such embeddings [41, Corollary 2.3.2].

Implementation and Results

We next demonstrate numerical results based on learning the map described in the equations (4)–(5) and then iterating it for forecasting. We realize g through a RNN of the type (1) with the causal embedding property. Regardless of how the map Γ is learnt and implemented, we call a system with a RNN that implements g in (4)–(5) as a recurrent conjugate network(RCN) since the dynamics of

the driven system's states produces a conjugacy to the input dynamical system as in (3). By setting the spectral radius of the matrix B to be 1 in (1), empirically, for α sufficiently small (and usually in $(0, 1)$) RNNs have the USP (see parameter-stability plot in [11]). The actual implementation of (4)–(5) is shown in the print in red in Fig. 1A.

In our RCN, we learn $\Gamma : (x_n, x_{n-1}) \mapsto u_n$ by learning a feedforward network (NN) on the principal components of states x_n . The use of principal components is taken only for an efficient state representation possibly to reduce the errors while learning and is not for approximation since all principal components are used. To be explicit, we denote the matrix with the first N states of the network data as row vectors by $X_{1:N}$. If $X_{1:N} = U\Sigma P^T$ denotes the singular value decomposition of $X_{1:N}$, then the principal component matrix is given by P and the principal components are given by $T_{1:N} = X_{1:N}P$. These principal components are used to train a feedforward neural network using the *Keras* library built on *Tensorflow*. If we denote the row vectors of $T_{1:N}$ by $t_i^T, i = 1, 2, \dots, N$ and the neural network by NN , then we learn the approximation $NN : (t_{n-1}, t_n) \mapsto \tilde{u}_n \approx u_n$. Consequently, an approximation of Γ is given by

$$NN \left(\begin{bmatrix} P^T x_{n-1} \\ P^T x_n \end{bmatrix} \right) = NN \circ \begin{bmatrix} P^T & 0 \\ 0 & P^T \end{bmatrix} \begin{bmatrix} x_{n-1} \\ x_n \end{bmatrix} \approx u_n.$$

The dynamical systems considered for prediction are an abstraction of complex behaviors in large-dimensional systems and detailed in [34]. The ability to reconstruct or forecast a dynamical system also relies on how an invariant density [42] which describe the statistical properties of the orbits are retained. The statistical G-test values are included in [34] to indicate the accuracy of retention of the statistical properties of the RCNs. The dynamical systems are chosen to exhibit different behaviors that often present a challenge for model reconstruction from data. The different behaviors chosen are turbulent behavior as in Lorenz system, a chaotic system without statistical stability as described by the linear response (e.g., [43]) as in the full logistic map, intermittency of a chaotic map in the H  non family as in [44], weak chaos and intermittency as in Pomeau- Manneville map [45]. We note that the logistic map and the Pomeau- Manneville map are both non-invertible, and hence the dynamics of the RCN could possibly be just semi-conjugate to the actual systems.

We consider the data from the Lorenz system and the full logistic map in Fig. 1 (B–F). A notable feature is that despite the very low sampling rate in Fig. 1B (step size of 0.1) in the discretization of the Lorenz system, the RCN is able to reconstruct the attractor. In Fig. 1F, despite the logistic map not having the linear response and also failing G -test [34] the simulated invariant density from the prediction of the Logistic map shows good resemblance. Due to the weighted sum of the inputs and states across nodes in a RNN like in (1), it is also empirically found to minimize the variance of the input noise while forecasting or attractor reconstruction as found in numerical simulations. This for instance is evident in Fig. 2A where the attractor seems to have lesser noise. Getting models that capture the statistical behavior for the data from the Pomeau-Manneville map (see Fig. 2F) is a challenge due to the weakly chaotic behavior that is a feature of some climatic models, and to the best of our knowledge, no machine learning algorithm has succeeded so far.

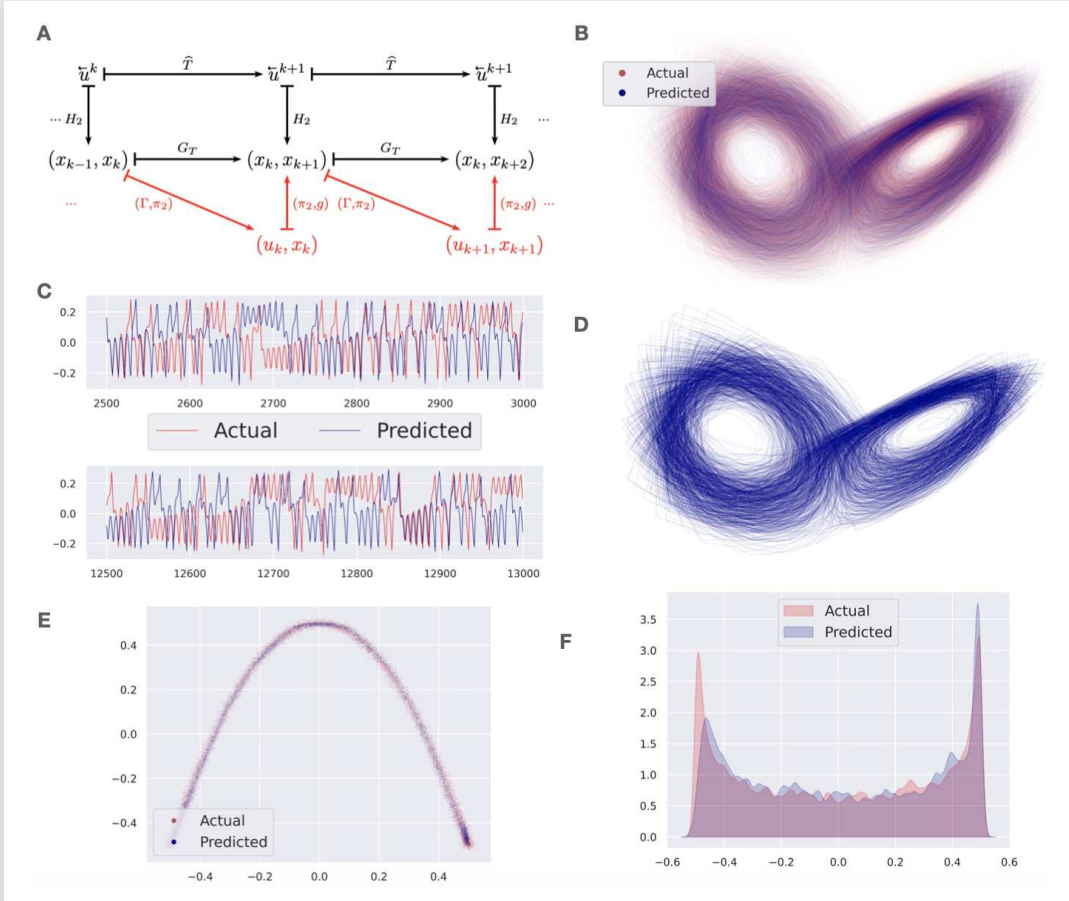


Fig. 1. The RCN used in generating the images is $g(u, x)$ as in (1) and the process of prediction is described in A. In all experiments, A and B were initialized randomly, with B having unit spectral radius. We used hyper-parameters $a = 0.5$ and $\alpha = 0.99$. We also used a 1000 dimensional network, i.e. $X = [-1, 1]^{1000}$. (B) Data (w_n) is generated from the Lorenz system, sampled every 0.1 timesteps. The input into the network is scaled down to fit inside $[-1, 1]^3$, and perturbed with noise. Specifically, the input (u_n) is given by $u_n = \frac{1}{100}w_n + \varepsilon_n$ where ε_n is normally distributed with 0 mean and standard deviation equal to 0.01. This translates to a signal to noise ratio of roughly 18dB. Training of Γ was accomplished using 2000 data points, after discarding the first 500 to allow the network to forget its initial state. Plotted is the result of the autonomous prediction of 50000 timesteps to showcase long term stability. (C, D) The samples (u_n) were generated in the same manner as in A, however instead of feeding in the full states, a sequence of observations was fed into the system. Although the theory is still conjectural for feeding such observations, the network still shows predictive capability. In this case the observations (u_n) is given by $u_n = \frac{1}{10} \left(\sin(\gamma w_x^{(n)}) + \sin(\gamma w_y^{(n)}) + \sin(\gamma w_z^{(n)}) \right)$, with $\gamma = 0.1$ intended to be a parameter to control the complexity of the observation. Plotted in C is the actual (red) and the predicted (blue) signals beginning at the time-step where prediction starts and after 12500 samples. Besides prediction, a map $\Gamma_{\text{full}} : (x_{n-1}, x_n) \mapsto \frac{1}{100}w_n$ was also learnt, used to reconstruct the full states of the Lorenz system out of the network as shown in D. This illustrated that although an obscured, lower-dimensional observation is fed into the RCN, the network contains all information. (E, F) Data (u_n) is generated from the full Logistic Map, then normalized to have zero mean, and perturbed with noise. Specifically, the input (u_n) is given by $u_n = w_n - \text{mean}(w) + \varepsilon_n$, where ε_n is normally distributed of zero mean and standard deviation equal to 0.01. This translates to a signal-to-noise ratio of roughly 30dB. Plotted is the phase portrait E and the smoothed invariant density F for actual (red) and predicted (blue) data, over 10000 prediction steps. Once again, training was accomplished with 2000 data steps after 500 had been discarded.

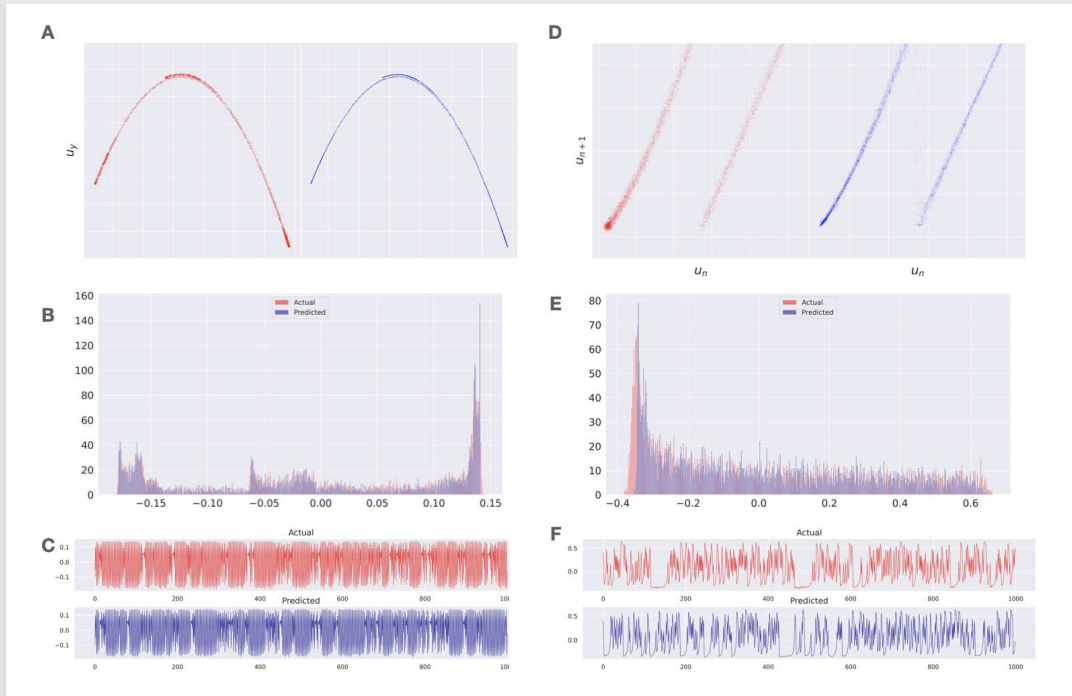


Fig. 2. The RCN setup is the same as in Figure 1. To capture intermittency in noisy data however, more training data was used: 1000 timesteps were discarded to allow the network to forget, and 5000 used for training. (A,B,C) Data (u_n) comes from an intermittent realisation from the Hénon family of maps. Specifically, $v_x^{(n+1)} = v_y^{(n)}$ and $v_y^{(n+1)} = -Jv_x^{(n)} + \mu - v_y^{(n)}$, with $J = 0.015$ and $\mu = 0.176$. Input (u_n) was normalized to have mean zero, scaled to fit inside $[-1, 1]^2$, and perturbed with noise. To be explicit, $u_n = \frac{1}{10}(v_n - \text{mean}(v)) + \varepsilon_n$ with ε_n normally distributed with zero mean and standard deviation equal to 0.001, resulting in a signal to noise ratio of 40dB. Plotted in A is the learnt (blue) and actual (red) attractors of the data. Observe that the predicted attractor show less noise than the input data. The figure B represents the learnt (blue) and actual (red) densities of the first coordinates of the data. Plotted in C showcases the first 1000 prediction steps of the v_y coordinate of the actual (red) and predicted (blue) data. (D,E,F) Data (u_n) comes from the Pomeau-Manneville family of maps. The update equation is given by $v_{n+1} = v_n(1 + 2^a v_n^a)$ if $0 \leq v_n < 0.5$ and $v_{n+1} = 2v_n - 1$ if $0.5 \leq v_n \leq 1$. For these results, $a = 0.6$ was used. Input (w_n) is given by $u_n = v_n - \text{mean}(v) + \varepsilon_n$ with ε_n distributed normally with zero mean and standard deviation equal to 0.01, roughly resulting in a signal to noise ratio of 26dB. Plotted in D is the phase portrait of the actual (red) and predicted (blue) data. Denoising is observed in the predicted attractor showing the two “hairpin” curves. Figure E showcases the learnt (blue) invariant density overlayed with the actual (red). Plotted in F is the trajectory of the actual (red) data and the predicted (blue) data.

Discussion

We have demonstrated how governing equations for data arising from the iterates of an unknown map can be obtained. In principle, if such temporal data is free of noise, and collected either directly or through a delay-coordinate map using an observable, then the temporal data can be embedded into a reconstruction space and the equations are exact.

Finding the set of observables of data that determine a less functionally complex learnable map so that its dynamics in the observed space gets closer to that of the action of the Koopman operator on the observables has been a pursuit for the last decade. In practice, however, the Koopman operators tend to have significantly more complicated spectral properties (e.g., non-isolated eigenvalues and/or continuous spectra) hindering the performance of data-driven approximation techniques. Here, we find that our equations determine observables for a dynamical system determined by the left-infinite history of the temporal data. At the heart of obtaining the equations, is that temporal data can be mapped into a new phase space through a driven (dynamical) system with the causal embedding property, and the single-lag dynamics in the new phase space is topologically conjugate to the system generating the input. Thus we achieve learning the action of the Koopman operator itself rather than approximating it.

Empirically it is found that the successive points in the temporal data in the driven system's phase space has a stronger linear relationship than the observed data when the dimension of the phase space is large enough. The functional complexity is empirically found to be much higher than produced through delay-embedding techniques. The long-term consistency of the learnt models is illustrated on chaotic maps, and data showing intermittency. The stability of forecasting against external noise is also observed.

The distinct advantage over other known data-driven approaches is that a driven dynamical system with the causal embedding property determines the observables for any dynamical system in its input space. This is remarkable since one does not have to resort to finding new observables or guessing the library of governing equations for new temporal datasets. Also, in contrast to driven systems presented in the reservoir computing paradigm, we show the existence of a learnable map. The driven system's proven properties of robustness to perturbations in the input, and also parameters in the system make them attractive for hardware implementations.

Acknowledgements We wish to thank Herbert Jaeger, Markus Haase, Igor Mezic for their helpful comments during the course of our work. The authors also thank the National Research Foundation for supporting research activities.

References

- [1] Majda AJ, Abramov R, Gershgorin B (2010) High skill in low-frequency climate response through fluctuation dissipation theorems despite structural instability. *Proceedings of the National Academy of Sciences* 107(2):581–586.
- [2] Ghil M, Lucarini V (2020) The physics of climate variability and climate change. *Reviews of Modern Physics* 92(3):035002.
- [3] Yule GU (1927) Vii. on a method of investigating periodicities disturbed series, with special reference to wolfer’s sunspot numbers. *Philosophical Transactions of the Royal Society of London. Series A, Containing Papers of a Mathematical or Physical Character* 226(636-646):267–298.
- [4] Takens F (1981) Detecting strange attractors in turbulence in *Dynamical systems and turbulence, Warwick 1980*. (Springer), pp. 366–381.
- [5] Principe JC, Rathie A, Kuo JM (1992) Prediction of chaotic time series with neural networks and the issue of dynamic modeling. *International Journal of Bifurcation and Chaos* 2(04):989–996.
- [6] Jaeger H, Haas H (2004) Harnessing nonlinearity: Predicting chaotic systems and saving energy in wireless communication. *science* 304(5667):78–80.
- [7] Lu Z, Hunt BR, Ott E (2018) Attractor reconstruction by machine learning. *Chaos: An Interdisciplinary Journal of Nonlinear Science* 28(6):061104.
- [8] Koopman B, Neumann Jv (1932) Dynamical systems of continuous spectra. *Proceedings of the National Academy of Sciences of the United States of America* 18(3):255.
- [9] Budišić M, Mohr R, Mezić I (2012) Applied koopmanism. *Chaos: An Interdisciplinary Journal of Nonlinear Science* 22(4):047510.
- [10] Manjunath G, Jaeger H (2013) Echo state property linked to an input: Exploring a fundamental characteristic of recurrent neural networks. *Neural computation* 25(3):671–696.
- [11] Manjunath G (2020) Stability and memory-loss go hand-in-hand: three results in dynamics and computation. *Proceedings of the Royal Society A* 476(2242):20200563.
- [12] Herteux J, Räth C (2020) Breaking symmetries of the reservoir equations in echo state networks. *Chaos: An Interdisciplinary Journal of Nonlinear Science* 30(12):123142.
- [13] Manjunath G (2020) An echo state network imparts a curve fitting. *Submitted*.
- [14] Wu Q, Fokoue E, Kudithipudi D (2018) On the statistical challenges of echo state networks and some potential remedies. *arXiv preprint arXiv:1802.07369*.
- [15] Faranda D, et al. (2019) Boosting performance in machine learning of turbulent and geophysical flows via scale separation.
- [16] Schmid PJ (2010) Dynamic mode decomposition of numerical and experimental data. *Journal of fluid mechanics* 656:5–28.

- [17] Williams MO, Kevrekidis IG, Rowley CW (2015) A data-driven approximation of the koopman operator: Extending dynamic mode decomposition. *Journal of Nonlinear Science* 25(6):1307–1346.
- [18] Brunton SL, Proctor JL, Kutz JN (2016) Discovering governing equations from data by sparse identification of nonlinear dynamical systems. *Proceedings of the national academy of sciences* 113(15):3932–3937.
- [19] Champion K, Lusch B, Kutz JN, Brunton SL (2019) Data-driven discovery of coordinates and governing equations. *Proceedings of the National Academy of Sciences* 116(45):22445–22451.
- [20] Brunton SL, Brunton BW, Proctor JL, Kaiser E, Kutz JN (2017) Chaos as an intermittently forced linear system. *Nature communications* 8(1):1–9.
- [21] Mezic I (2020) Koopman operator, geometry, and learning. *arXiv preprint arXiv:2010.05377*.
- [22] Sauer T, Yorke JA, Casdagli M (1991) Embedology. *Journal of statistical Physics* 65(3):579–616.
- [23] Stark J (1999) Delay embeddings for forced systems. i. deterministic forcing. *Journal of Nonlinear Science* 9(3):255–332.
- [24] Robinson JC (2010) *Dimensions, embeddings, and attractors*. (Cambridge University Press) Vol. 186.
- [25] Gutman Y, Qiao Y, Szabó G (2018) The embedding problem in topological dynamics and takens’ theorem. *Nonlinearity* 31(2):597.
- [26] Baraniuk RG, Wakin MB (2009) Random projections of smooth manifolds. *Foundations of computational mathematics* 9(1):51–77.
- [27] Eftekhari A, Yap HL, Wakin MB, Rozell CJ (2018) Stabilizing embedology: Geometry-preserving delay-coordinate maps. *Physical Review E* 97(2):022222.
- [28] Yair O, Talmon R, Coifman RR, Kevrekidis IG (2017) Reconstruction of normal forms by learning informed observation geometries from data. *Proceedings of the National Academy of Sciences* 114(38):E7865–E7874.
- [29] Ingram WT, Mahavier WS (2011) *Inverse limits: From continua to Chaos*. (Springer Science & Business Media) Vol. 25.
- [30] Puccetti G (2019) Measuring linear correlation between random vectors. *Available at SSRN 3116066*.
- [31] Appeltant L, et al. (2011) Information processing using a single dynamical node as complex system. *Nature communications* 2:468.
- [32] Kudithipudi D, Saleh Q, Merkel C, Thesing J, Wysocki B (2016) Design and analysis of a neuromemristive reservoir computing architecture for biosignal processing. *Frontiers in neuroscience* 9:502.

- [33] Vandoorne K, et al. (2014) Experimental demonstration of reservoir computing on a silicon photonics chip. *Nature communications* 5:3541.
- [34] (2021). *Supplementary Material that is available online along with this publication.*
- [35] (2020). *Embedding Information onto a Dynamical System.*
- [36] Grigoryeva L, Ortega JP (2018) Echo state networks are universal. *Neural Networks* 108:495–508.
- [37] Korda M, Putinar M, Mezić I (2020) Data-driven spectral analysis of the koopman operator. *Applied and Computational Harmonic Analysis* 48(2):599–629.
- [38] Manjunath G, Jaeger H (2014) The dynamics of random difference equations is remodeled by closed relations. *SIAM Journal on Mathematical Analysis* 46(1):459–483.
- [39] Eisner T, Farkas B, Haase M, Nagel R (2015) *Operator theoretic aspects of ergodic theory.* (Springer) Vol. 272.
- [40] Grigoryeva L, Hart A, Ortega JP (2020) Chaos on compact manifolds: Differentiable synchronizations beyond takens. *To appear in Physical Review E: arXiv preprint arXiv:2010.03218.*
- [41] Hart A, Hook J, Dawes J (2020) Embedding and approximation theorems for echo state networks. *Neural Networks.*
- [42] Lasota A, Mackey MC (2013) *Chaos, fractals, and noise: stochastic aspects of dynamics.* (Springer Science & Business Media) Vol. 97.
- [43] Baladi V (year?) Linear response, or else. III.
- [44] Kaplan H (1993) Type-i intermittency for the h enon-map family. *Physical Review E* 48(3):1655.
- [45] Pomeau Y, Manneville P (1980) Intermittent transition to turbulence in dissipative dynamical systems. *Communications in Mathematical Physics* 74(2):189–197.